HHS Public Access

Author manuscript

Mol Psychiatry. Author manuscript; available in PMC 2021 October 13.

Published in final edited form as:

Mol Psychiatry. 2021 July ; 26(7): 3461–3475. doi:10.1038/s41380-020-0840-3.

Optogenetic manipulation of an ascending arousal system tunes cortical broadband gamma power and reveals functional deficits relevant to schizophrenia

James M. McNally, PhD[1,*], **David D. Aguilar, PhD**[1], **Fumi Katsuki, PhD**[1], **Leana Radzik**[2], **Felipe L. Schiffino, PhD**[1], **David S. Uygun, PhD**[1], **James T. McKenna, PhD**[1], **Robert E. Strecker, PhD**[1], **Karl Deisseroth, MD PhD**[3], **Kevin M. Spencer, PhD**[4], **Ritchie E. Brown**, **Dr Rer Nat**[1]

[1)]VA Boston Healthcare System and Harvard Medical School, Dept. of Psychiatry, West Roxbury, MA, USA.

[2)]Stonehill College, Dept. of Neuroscience, Easton, MA USA.

[3)]Stanford University, Psychiatry and Behavioral Sciences/Bioengineering, Stanford, CA, USA

[4)]VA Boston Healthcare System and Harvard Medical School, Dept. of Psychiatry, Jamaica Plain, MA, USA.

Abstract

Increases in broadband cortical electroencephalogram (EEG) power in the gamma band (30–80 Hz) range have been observed in schizophrenia patients and in mouse models of schizophrenia. They are also seen in humans and animals treated with the psychotomimetic agent ketamine. However, the mechanisms which can result in increased broadband gamma power and the pathophysiological implications for cognition and behavior are poorly understood. Here we report that tonic optogenetic manipulation of an ascending arousal system bi-directionally tunes cortical broadband gamma power, allowing on-demand tests of the effect on cortical processing and behavior. Constant, low wattage optogenetic stimulation of basal forebrain (BF) neurons containing the calcium-binding protein parvalbumin (PV) increased broadband gamma frequency power, increased locomotor activity, and impaired novel object recognition. Concomitantly, task-associated gamma band oscillations induced by trains of auditory stimuli, or exposure to novel objects, were impaired, reminiscent of findings in schizophrenia patients. Conversely, tonic optogenetic inhibition of BF-PV neurons partially rescued the elevated broadband gamma power elicited by subanesthetic doses of ketamine. These results support the idea that increased cortical broadband gamma activity leads to impairments in cognition and behavior and identify BF-PV activity as a modulator of this activity. As such, BF-PV neurons may represent a novel target for

[*]**Corresponding author: James M. McNally, PhD**., Department of Psychiatry, VA Boston Healthcare System-Harvard Medical School, West Roxbury, MA 02132, Phone: 857-203-4369, James_McNally@hms.harvard.edu.

Conflict of Interest Statement

The authors declare no competing financial interests. JTM received partial salary compensation and funding from Merck MISP (Merck Investigator Sponsored Programs) but has no competing financial interest with this work.

Supplementary information is available at MP's website

pharmacotherapy in disorders such as schizophrenia which involve aberrant increases in cortical broadband gamma activity.

INTRODUCTION

Normal cortical function relies on the ability of neural networks to maintain stable, yet flexible, levels of activity. This process is precisely regulated by the ratio of activity in the excitatory and inhibitory components of the cortical circuitry (**E/I balance**). Altered cortical E/I balance has been suggested to play a central role in the pathophysiology of numerous neuropsychiatric disorders, including schizophrenia, and has been linked to cognitive, negative, and positive symptoms (1–4). Thus, there is intense interest in revealing the mechanisms which regulate E/I balance, understanding the consequences of disrupted E/I balance, and designing therapeutic interventions which can restore E/I balance in disrupted cortical circuits.

Electroencephalographic (**EEG**) power in the gamma band range (30–80 Hz or higher) is a common metric employed to assess E/I balance (5–7). Increased resting broadband gamma activity has been observed in individuals with schizophrenia-spectrum disorders and correlated with symptoms (8–12). Similarly, in both human and animal studies, the psychotomimetics ketamine and phencyclidine increase cortical broadband gamma band power (13–18) presumably by inhibiting NMDA receptors on cortical interneurons, leading to cortical excitation via disinhibition of pyramidal neuron activity [(19,20) but see (21,22)]. Mouse genetic models of schizophrenia also report an increase in spontaneous broadband gamma band power (21–23). Thus, convergent evidence suggests that increased broadband gamma power is an important feature of schizophrenia. However, the consequences of increased broadband gamma power on cortical function and behavior remain poorly understood and the neuronal circuits which can be targeted to recalibrate this activity are an open area of investigation.

The basal forebrain (**BF**) has been suggested to represent a potent regulator of cortical high-frequency EEG activity (24–28). Furthermore, gamma band activity in BF is correlated with cortical gamma (29,30). Thus, alterations in the activity of BF neurons are one possible cause of disease-related alterations in cortical gamma activity. While cholinergic BF systems have been extensively studied, the contribution of non-cholinergic BF projection systems are just beginning to be uncovered (31–34). Previously, we showed that strong *phasic* optogenetic excitation of one population of GABAergic projection neurons, BF parvalbumin (**PV**) neurons, elicited synchronous *narrow-band* cortical *oscillations*, with a preference for the gamma frequency range, likely mediated via the projections of BF-PV neurons to cortical PV interneurons (33). Here, we report the effect of a different optogenetic stimulation paradigm, designed to increase the natural discharge rate of BF-PV neurons and increase cortical broadband gamma activity. We use this paradigm to test the pathophysiological effects of increased or decreased cortical broadband gamma power, produced by manipulation of the activity of a specific subcortical arousal system, the BF-PV neurons.

We find that *tonic* optical stimulation of BF-PV neurons in mice increases cortical *broadband* gamma power. This increased broadband gamma activity was associated with electrophysiological and behavioral phenotypes associated with schizophrenia, including increased locomotor activity, impairments in task-associated gamma oscillations, and novel object recognition. Conversely, tonic inhibition of BF-PV neurons partially reverses increases in broadband gamma power caused by the psychotomimetic, ketamine. These results demonstrate that BF-PV neurons play an important role in the control of both resting broadband gamma activity and task-associated narrow band gamma oscillations. The findings also link gamma power changes with functional deficits seen in patients with schizophrenia, thereby identifying BF-PV neurons as a potential therapeutic target.

METHODS AND MATERIALS

Subjects:

Adult (>4 months) PV-cre mice (Jackson Labs, Bar Harbor, Maine; Stock No. 008069) were housed at 21°C with 12:12 hour light/dark cycle (lights-on 7:00AM), and food and water available *ad libitum*. All procedures were performed in accordance with National Institutes of Health guidelines and were approved by the VA Boston Institutional Animal Care and Use Committee. Both male and female mice were used in this study.

Viral Vectors:

Optogenetic experiments employed double-floxed adeno-associated viral vectors (AAV) with Cre-dependent expression of channelrhodopsin2 (AAV5-DIO-CHR2-EYFP) or Archaerhodopsin subtype TP003 (AAV5-CAG-FLEX-Arch-GFP) for excitation or inhibition of BF-PV neurons respectively, purchased from the University of North Carolina (UNC) Vector Core. Validation of targeting/expression of viral transduction, functional efficacy of these vectors in exciting or inhibiting BF-PV neurons and fiberoptic cannula implantation were performed as described previously (33).

Stereotaxic Surgeries:

Under isoflurane anesthesia (induction, 5%; maintenance, 1–2%), mice were injected bilaterally with 1 μL (50 nL/min) of AAV-ChR2 or AAV-ArchT using a Hamilton syringe (75N; 30G needle). Injections targeted the magnocellular preoptic area (MCPO)/Horizontal limb of the diagonal band (HDB) region of the BF (AP 0.0 mm from bregma; ML 1.6; DV −5.2) where cortically-projecting PV neurons are concentrated (19). Following experiments, correct targeting of AAV injections was histologically validated (Supplementary Figure 1). Two weeks following AAV viral injections, mice underwent a second surgical procedure to implant EEG screw electrodes (0.10”, Cat No. 8403, Pinnacle Technology Inc.) bilaterally above frontal cortex (AP 1.5 mm; ML ±1 mm). Reference and ground screws were placed in the bone above the midline cerebellum and parietal cortex, respectively. Electromyography (EMG) electrodes were placed in the nuchal muscle. All electrodes were connected to a headmount (Cat No. 8402, Pinnacle Technology Inc.). Fiber-optic cannulae (200μm, 0.22 NA optical fiber, Doric Lenses) were bilaterally implanted targeting BF (AP 0; ML ±1.6, DV −5.4). Each mouse was allowed to recover from surgery for at least one week prior to experiments.

In Vivo Electrophysiology:

EEG/EMG signals were amplified using a 3 Channel-EEG System (#8200-K1-SL, Pinnacle Technologies). Signals were recorded (2000 Hz sampling rate) with a secondary digitizer (Digidata 1440, Molecular Devices) using WinWCP software (John Dempster, University of Strathclyde), to both record EEG/EMG and generate TTL output signals to control stimuli. Auditory stimulation used in the ASSR task consisted of trains of white noise clicks (10ms) and were delivered via a cage mounted speaker. ChR2 stimulation or ArchT inhibition was performed using a blue laser (473nm; Model No CL473–050-O or DL473–80-O, CrystaLaser), or green laser (532nm; MGL-III-543/1~100mW, OptoEngine), respectively. Light was delivered via fiber-optic patch cables (MFP_50/125/900–0.22_10mm_FC-ZF1.25, Doric lenses), connected to the implanted optical cannulae. Optimal laser power for tonic stimulation was chosen based on initial dose-finding experiments to maximize effects on broadband gamma [n=3; 3mW: −1.9 ± 5.0%; 4mW: 20.0 ± 4.7%; 5mW: 39.26 ± 17.4%; 6mW: 6.82 ± 4.0%]. Here, we observed an inverted U-shaped dose response pattern, with a laser power of 5mW producing the maximal effect on broadband gamma. Using the Deisseroth laboratory on-line calculator (https://web.stanford.edu/group/dlab/cgi-bin/graph/chart.php), assuming no light leakage, this laser power would produce a predicted irradiance in the brain of 8.7 mW/mm^2 at 0.5 μm from the fiber tip and 1.8 mW/mm^2 at 1 μm from the tip. However, these values may underestimate the spatial extent of the effects of stimulation since BF PV neurons appear to be connected by electrical synapses (35). Control experiments showed that ChR2 stimulation and ArchT inhibition parameters used in this study did not result in stimulation site tissue damage (Supplementary Figure 2).

To analyze the data, time-frequency spectral analysis was performed on raw EEG records, and the resulting spectra were averaged. Mock stimulation (control) experiments were performed in the same manner as those with optical stimulation, but with the laser turned off. Additionally, control mice were not virally injected, and received laser light stimulation alone. For acute ketamine (Ketalar, JHP Pharmaceuticals) treatment, mice were injected (i.p) at dose of 15 mg/kg. All results were analyzed within animal.

Behavioral Tasks:

To assess locomotor activity, experiments were performed on three consecutive days in an open field environment (26cm × 48cm). On day one, mice were habituated to the environment for 10 minutes (no recording/stimulation performed). Days two and three consisted of either a control or optogenetic stimulation (counterbalanced). Movement was tracked via video monitoring. A custom-designed workflow utilizing open source software (Bonsai, OpenEphys.org) was used to assess locomotor activity under each condition. For the novel object recognition (**NOR**) task, mice were first habituated to the NOR chamber (44 × 44 cm) for 10 minutes with no objects presented. EEG/EMG was recorded during task performance. All mice performed the task with and without receiving optogenetic stimulation (counterbalanced). An automated on-line video tracking system (EthoVision XT, Noldus Information Tech.) was used to timestamp EEG records with investigation timepoints (manually confirmed post-hoc) and to analyze behavioral performance. This system increased throughput and allowed us to mitigate experimenter bias, as no blinding protocol was employed. For investigation associated EEG data, multi-taper spectral analysis

(36) was performed on 6 second segments of EEG data (2 seconds pre- & 4 seconds post-investigation). The power values in the time frequency spectra from each investigation were then normalized to the mean power in each frequency bin across the 2 seconds preceding the investigation. These normalized spectra of total power for each investigation were then averaged across all mice for each phase of the task. For statistical analysis of this data, power across the frequency band of interest (25 – 58Hz) for each 6s EEG segment was binned (250ms) and values compared between treatment groups using a repeated measure analysis of variance (RMANOVA). We chose to focus on this frequency range based on a prior study which suggested that activity in the 25–58 Hz range reflects top-down predictive coding during a spatial working memory test (37), and our own control data in the NOR task showing prominent increases in power in this range associated with object investigation.

Data and Statistical Analyses:

Data were analyzed offline using custom scripts written for MATLAB (R2016a-2018b, MathWorks). Analysis of spectral power and/or phase was performed using either the multi-taper method ((36); Chronux Toolbox, Chronux.org), or complex Morlet wavelet analysis, as described previously (11). All data are presented as mean ± standard error. Statistical analyses were performed using both JMPpro12 (SAS Institute Inc.) and R (www.r-project.org). RMANOVA were performed using Tukey's HSD post hoc test, and repeated measures correlation were performed in the manner described by Bakdash and Marusich (38). For NOR, univariate t-tests were used to compare object exploration to the chance level of exploration ($\mu = 50\%$; prob > t), and student's t-test were used to test between groups.

RESULTS

Tonic Optogenetic Stimulation of BF-PV Neurons Enhances Broadband Gamma Band Activity but Impairs Evoked Gamma Oscillations

Here we employed a "tonic" stimulation paradigm, where mice expressing ChR2 bilaterally in BF-PV neurons were treated with constant low wattage (5 mW) light for 60 s, repeated at 5-minute intervals (10 repetitions). This tonic stimulation paradigm progressively increased broadband gamma band power during stimulation, with a slow (>60s) return to baseline levels following the end of stimulation (Figure 1B&D). Comparing the power spectra of EEG activity from the 60 s before stimulation to that occurring during the stimulation period (Figure 1C), we observed an elevation in broadband gamma power only in mice expressing ChR2, and not in control animals which received laser stimulation alone [Figure 1D&E; ChR2+: n=12 (8 ♂ 4♀); +44.3 ± 10.5%; ChR2-: n=8 (5 ♂ 3♀); +8.0 ± 5.0%; t-test: $t_{18} = -2.67$, $p = 0.02$]. Other frequency bands were not significantly altered.

Patients with schizophrenia exhibit well-replicated deficits in their ability to synchronize cortical firing in response to repetitive auditory stimuli delivered at 40 Hz, the so-called "auditory steady state response" (**ASSR**) (11,39–42). One potential explanation of this abnormality is enhanced background discharge of cortical principal neurons ('noise') resulting from reduced activity in cortical PV interneurons. Thus, we tested whether increased broadband activity produced by tonic BF-PV optogenetic stimulation would affect

ASSR. Mice with bilateral BF-PV expression of ChR2 [n=6(4 ♂ 2♀)] were exposed to 1 s trains of auditory clicks (90 dB) delivered at 40 Hz and repeated every 2 s. ASSR was assessed from 3 consecutive blocks of stimulation, each consisting of 100 repetitions. The initial block, auditory stimulation alone, provided a baseline response. For the second block, auditory stimulation was coupled with tonic stimulation of BF-PV neurons (5 min; 5 mW). A third block of auditory stimulation was used to assess recovery. Wavelet analysis of frontal cortex EEG determined the effects on evoked power and phase-locking factor.

As shown in Figure 2 (A&B), the relative change (fold change from background) in 40 Hz stimulus-evoked power (40 ± 2 Hz) was significantly decreased with tonic BF-PV stimulation compared to both baseline and recovery periods [RMANOVA, $F_{2,10} = 6.06$, $p = 0.02$, Baseline: 7.23 ± 1.22, ChR2: 3.32 ± 0.73, Recovery: 7.72 ± 1.91; Baseline vs. ChR2: $p = 0.02$, Recovery vs. ChR2: $p = 0.04$]. Further analysis revealed a significant elevation in pre-auditory stimulus (0–0.8s) 40 Hz total power with ChR2 stimulation compared to the baseline, and a trend-level increase compared to recovery [Figure 2C; RMANOVA, $F_{2,10} = 5.09$, $p = 0.03$, Baseline: 40.96 ± 4.41 μV^2/Hz, ChR2: 59.45 ± 7.15 μV^2/Hz, Recovery: 39.07 ± 4.00 μV^2/Hz; Baseline vs. ChR2: $p = 0.04$, Recovery vs. ChR2: $p = 0.06$]. Additionally, there was a significant decrease in absolute evoked power during the ASSR (1.2 – 2 s) with BF-PV stimulation [Figure 2D; RMANOVA, $F_{2,10} = 10.04$, $p = 0.004$, Baseline: 302.09 ± 59.60 μV^2/Hz, ChR2: 192.90 ± 42.69 μV^2/Hz, Recovery: 292.40 ± 67.61 μV^2/Hz; Baseline vs. ChR2: $p = 0.03$, Recovery vs. ChR2: $p = 0.05$]. The relationship between the 40 Hz ASSR evoked power and the pre-auditory stimulus broadband gamma power was in the expected direction but did not show a significant correlation (Supplementary Figure 3A; repeated measures correlation, $r = -0.36$, $p = 0.22$).

Another common measure in clinical ASSR studies looks at event-related consistency, or phase-locking at 40 Hz. Here, phase values were first derived via wavelet analysis for each trial. Circular variance across trials was then calculated to yield the phase-locking factor (**PLF**). The mean PLF at 40 ± 2 Hz was then calculated across the 3 s ASSR epoch (Figure 2E–G) for each animal (n=6). Repeated measures ANOVA ($F_{2,10} = 10.04$, $p = 0.004$, Baseline: 0.16 ± 0.01; Tonic Stim.: 0.13 ± 0.01; Recovery: 0.19 ± 0.02) showed a significant decrease in ASSR PLF with tonic BF-PV stimulation compared to the baseline and recovery periods ($p=0.04$ and $p=0.003$ respectively). Additionally, we observed a significant negative correlation between 40 Hz PLF and pre-auditory stimulus broadband gamma power (Supplementary Figure 3B; repeated measures correlation, $r = -0.64$, $p = 0.02$). Together, these findings demonstrate that tonic stimulation of BF-PV neurons elevates background gamma power and impairs evoked 40 Hz gamma band oscillations, reminiscent of clinical and computational modeling studies of schizophrenia (9,11,22,40,43–45).

In addition to the steady-state component of ASSR, we examined the onset event-related potential (ERP), which occurred during the first 200ms of the auditory stimulus train (1–1.2s). Here, we examined both the amplitude of N1 component of the onset ERP, as well as stimulus-evoked broadband gamma power (Supplementary Figure 4). The N1 peak was not significantly affected by tonic BF-PV stimulation when compared to baseline but was reduced compared to the recovery phase of the task [RMANOVA, $F_{2,10} = 4.11$, $p = 0.04$, Baseline: 104.17 ± 16.15 μV, ChR2: 89.60 ± 9.17 μV, Recovery: 123.67 ± 10.96 μV;

Baseline vs. ChR2: p = 0.46, Recovery vs. ChR2: p = 0.04, Baseline vs. Recovery: p = 0.28]. A similar result was observed when measuring the relative change (fold change from background) in broadband gamma associated with the onset ERP [RMANOVA, $F_{2,10} = 5.83$, p = 0.02, Baseline: 1.30 ± 0.06, ChR2: 1.27 ± 0.04, Recovery: 1.43 ± 1.06; Baseline vs. ChR2: p = 0.82, Recovery vs. ChR2: p = 0.02, Baseline vs. Recovery: p = 0.06]. Together, these results suggest a rebound effect specific to the onset ERP, which was not observed in the steady-state component of the ASSR.

Optogenetic Stimulation of BF-PV Neurons Increases Locomotor Activity

Increased locomotor activity is commonly observed in animals treated with psychotomimetics which increase broadband gamma activity, such as the NMDA receptor antagonist ketamine. To determine if tonic BF-PV stimulation would have a similar impact on behavior, we assessed locomotor activity in mice in both the presence and absence of tonic stimulation of BF-PV neurons. Following habituation, mice were given 10 minutes to explore an open field environment. Mouse movement was tracked via video monitoring for the last five minutes of this exploration opportunity. Animals received tonic BF-PV stimulation during this 5-minute period (30–180 s) on one day, and mock stimulation (no laser) on the other as a control. As shown in Figure 3, all mice with BF-PV expression of ChR2 [n=8(5 ♂ 3♀)] showed a significant increase in total distance traveled with tonic stimulation of BF-PV neurons, compared to mock stimulation [Stim: 1518.8 ± 329.1 cm; Con: 967.3 ± 184.8 cm; paired t-test: $t_7 = 3.31$, p=0.01]. The cumulative distance plot of mouse locomotor activity shows that the increase in movement seen in ChR2 expressing mice is associated with the time that the tonic stimulation was given (Figure 3 D&E). Increased locomotor activity was not observed in mice without ChR2 expression [n=7(4 ♂ 3♀); Stim: 1034.8 ± 121.1 cm; Con: 889.4 ± 97.8 cm, paired t-test: $t_6 = 1.59$, p>0.05]. Direct comparison of the increase in locomotor activity to elevation in broadband gamma elicited by tonic BF-PV stimulation revealed a modest but highly significant positive correlation (Supplementary Figure 5). However, following stimulation the time course of the cessation of elevated locomotor activity appears to be far more rapid that that of the elevation in broadband gamma, suggesting these effects are at least partially separable.

Optogenetic Stimulation of BF-PV Neurons Impairs Novel Object Recognition (NOR) Performance and Object Investigation induced Gamma Activity

We next examined the effects of tonic BF-PV stimulation on the NOR task, a cognitive paradigm used to assess recognition memory (46). The task consisted of two phases (Figure 4A); the familiarization phase (5 min) where two identical objects were presented, and the recall phase (10 min) where one of the familiar objects was replaced with a novel object. There was a 10-minute retention interval between the familiarization and recall phases of the task. All mice (n=10(8 ♂ 2♀)) performed the task two times: once without optogenetic stimulation (Con), and once with tonic BF-PV stimulation given during the familiarization phase (Stim). These task repetitions were separated by at least 1 week and were performed using different objects, which had been determined to have equivalent salience.

As shown in Figure 4B, during the familiarization phase of the task, object preference was not significantly different from chance [% investigation time(Con: 55 ± 5%, $t_9 = 0.89$, p

= 0.19; Stim: 46 ± 4%, t_9 = −0.91, p = 0.81); % total Investigations (Con: 55 ± 4%, t_9 = 1.19, p = 0.13; Stim: 48 ± 4%, t_9 = −0.42, p = 0.66)]. By contrast, during the recall phase of the task, novel object preference was only observed in control recordings and not in experiments where mice received BF-PV stimulation during the familiarization phase. [% investigation time (Con: 67 ± 6%, t_9 = 3.03, p = 0.01; Stim: 40 ± 7%, t_9 = −1.50, p = 0.91); % total investigations (Con: 60 ± 6%, t_9 = 1.59, p=0.09; Stim: 38 ± 7%, t_9 = −1.78, p = 0.95)]. Further, both of these measures significantly differed between the two groups (% time spent: t_{18} = −3.10, p = 0.01; % total investigations: t_{18} = −2.39, p = 0.03). To ensure the above effects were not related to context specific learning, in a subset of these mice (n = 6) we additionally examined the effects of BF-PV stimulation during both phases of the task. Using this stimulation paradigm, no significant novel object preference was observed during the recall phase [% investigation time (57 ± 10%, t_5 = 0.72, p = 0.25); % total investigations (53 ± 7%, t_5 = 0.45, p = 0.33)].

Similar to the open field locomotor findings reported above, tonic BF-PV stimulation significantly enhanced total distance traveled (Con: 1009 ± 63 cm; Stim: 1535 ± 67 cm; p < 0.01) and velocity (Con: 3.15 ± 0.20 cm/s; Stim: 4.80 ± 0.21 cm/s; p < 0.01) during task performance (Figure 4C). Additionally, stimulation significantly increased the total number of object investigations of both objects (Con: 23.1± 2.2; Stim: 60.8 ± 6.6 cm; p < 0.01) and the combined investigation time for both objects (Con: 19.4 ± 2.7 s; Stim: 49.0 ± 6.1 s; p < 0.01) during the familiarization phase of the task. These effects were absent during the recall phase of the task in the absence of optical stimulation [Total distance (Con: 1488 ± 235 cm; Stim: 1632 ± 175 cm; p>0.05); Velocity (Con: 2.65 ± 0.31 cm/s; Stim: 2.66 ± 0.27 cm/s; p>0.05); Total Investigation # of both objects (Con: 43.8 ± 8.2; Stim: 48.2 ± 5.8; p>0.05); Combined Investigation time for both objects (Con: 42.9 ± 10.4s; Stim: 35.6 ± 5.6s; p>0.05)].

Throughout all phases of task performance, on-line tracking of nose position was employed to extract frontal EEG activity related to investigations of the object that remained unchanged across both phases of the task. Time frequency analysis was then performed for EEG data associated with each investigation (total power), with the results normalized to the power of the prior 2 seconds of baseline EEG activity. Results were then pooled across all experimental mice for each experimental condition and task phase (Figure 4 D&E). As shown in Figure 4E, during the familiarization phase of the task, investigation of objects was associated with short bursts of low frequency gamma band activity (25–58Hz). This phenomenon was significantly impaired when mice received tonic BF-PV stimulation. During the recall phase of the task, the investigation induced gamma response was restored to control values in the mice that had been treated with BF-PV stimulation during the familiarization phase. Examining the relationship between pre-investigation broadband gamma power to investigation induced low frequency gamma for all object investigations recorded showed a small but highly significant negative correlation (Supplementary Figure 6A; repeated measures correlation, induced gamma versus normalized background gamma, r = −0.28, p = 9.9e-11), supporting the idea that higher background broadband gamma leads to a smaller exploration induced response. Further, comparison of the average investigation induced gamma response observed in the ***familiarization*** phase of the task to novel object

preference during the ***recall*** phase showed a strong positive correlation (Supplementary Figure 6B & C; repeated measures correlation, gamma versus % time investigating, r = 0.85, p = 0.01 & gamma versus % number of investigations, r = 0.75, p = 0.01). This suggests that the impairment in exploration-induced gamma response to ***initial*** object investigation is related to impaired novel object preference.

Optogenetic Rescue of Ketamine Induced Elevation in Broadband Gamma

Finally, we investigated whether inhibition of BF-PV activity could correct increased broadband gamma power induced by a psychotomimetic. To test this, BF-PV neurons [n=8(5 ♂ 3♀)] were bilaterally transduced with the inhibitory opsin, ArchT, allowing optogenetic silencing of their activity (33). Five minutes into a 60-minute recording, mice received an acute, subanesthetic dose of ketamine (15 mg/kg). After allowing 5 minutes for the ketamine to take effect, mice received either tonic bilateral optogenetic inhibition of BF-PV neurons (5 min constant 532 nm light; 20 mW) or mock stimulation (counterbalanced, treatments 1 week apart). As predicted by previous work (13,47), acute injection of ketamine rapidly elevated broadband gamma band power (Figure 5). During the 5-minute period of mock inhibition (No Laser, 10–15 min, Figure 5A) ketamine elicited a 59.4 ± 11.8% increase in broadband gamma power above baseline (pre-ketamine; 0–5 min). During the same time period, with concurrent ArchT inhibition of BF-PV neurons (Figure 5B), this increase in broadband gamma power was reduced to 33.8 ± 4.8%. Overall, optogenetic BF-PV inhibition led to a statistically significant decrease in the elevation of gamma band power elicited by ketamine (−36.81 ± 8.4%; p=0.02, Figure 5C). ArchT inhibition of BF-PV neurons alone, in the absence of ketamine, did not significantly affect broadband gamma band power in the frontal cortex EEG (−1.3 ± 5.8% change from baseline).

DISCUSSION

Increasing evidence supports the critical role of cortical E/I balance in the regulation of cortical network activity. Abnormalities in this balance, reflected by elevated broadband gamma activity, represent an important feature of the etiology of schizophrenia and other neuropsychiatric disorders (2,4,48,49). Here we show that manipulation of the activity level of BF-PV projection neurons can bidirectionally tune cortical broadband gamma activity, leading to altered task-associated gamma band activity and changes in behavior reminiscent of both electrophysiological and behavioral phenotypes associated with schizophrenia. Furthermore, bilateral optogenetic inhibition of BF-PV neurons partially rescued the increase in spontaneous gamma power elicited by ketamine, identifying BF-PV neurons as a possible therapeutic target for treatment of psychosis.

One of the principal roles of the BF is to regulate cortical activity levels (50–53). Direct stimulation or inhibition of BF firing enhances or slows activity in cortical EEG, respectively (25,31–34,54) and enhances responsiveness to sensory input (55). While BF cholinergic neurons have been classically implicated in the augmentation of cortical activation, recent findings suggest that GABAergic BF neurons also play an important role (31–34). The results presented here show that elevations of the discharge of BF-PV neurons via low-wattage tonic optogenetic activation increases cortical broadband gamma

activity mimicking the pathophysiological increases in broadband gamma activity observed in rodent models of schizophrenia, suggesting that BF-PV neurons may be important in regulating such activity. Prior studies have observed that BF-PV neurons show limited local connectivity (31). Thus, the effects observed in our present work are more likely to be mediated by extra-BF projections. Beyond direct projections to the cortex, BF-PV also strongly project to the thalamic reticular nucleus (56), so increasing BF-PV neuron activity could also lead to disinhibition of thalamocortical relay neurons, and as a result promote increased broadband gamma in the cortex. Supporting this idea, chemogenetic activation of glutamatergic thalamocortical neurons similarly increases high-frequency cortical activity (32).

Prior theoretical and experimental studies have hypothesized that enhanced broadband gamma band activity could interfere with cortical information processing (8,11,22,57–59). One example is impaired task-evoked gamma band activity in response to the 40Hz ASSR; a widely-replicated finding in schizophrenia patients (39,40). One possible explanation of the ASSR deficit observed in schizophrenia patients is that an increase in background activity or “noise” in the cortex impairs entrainment of principal neurons to the steady-state response (11,12,22,44,60). Our findings support this hypothesis, since both the power and phase locking of the ASSR to 40 Hz auditory stimuli was reduced with increases in broadband gamma activity induced by tonic BF-PV stimulation. Further, 40 Hz phase locking showed a significant negative correlation with increased pre-stimulus broadband gamma power, as observed in schizophrenia patients (11). While this clinical study did not observe the resting-state alterations in broadband gamma activity reported here, the work examined patients with chronic schizophrenia. Recently, it has been suggested that elevated resting-state broadband gamma is evident in clinically high risk individuals, and first-episode schizophrenia patients (9). Therefore, our results may be more relevant to the early stages of schizophrenia.

In this study, we also examined the onset ERP associated with the 40 Hz ASSR. Reductions of the N1 component of auditory evoked ERPs have been consistently reported in patients with schizophrenia (61,62), and have been proposed as a marker of functional brain abnormalities related to the genetic predisposition to schizophrenia (63). Here, although stimulation tended to reduce this response compared to baseline, the effect was variable and did not reach significance. However, the response during optical stimulation was reduced compared to the recovery phase of the task, following cessation of tonic BF-PV stimulation, measured in terms of both broadband gamma power and N1 peak amplitude. Interestingly, N1 amplitude has been observed to be influenced by several factors, including arousal level, and attention. Changes in E/I balance likely will be reflected by changes in arousal, another related but separate function of BF-PV neurons (64). Thus, we theorize that this higher response during the recovery period may be associated with a lasting impact on attention/arousal following tonic BF-PV stimulation, an effect which takes several seconds to manifest itself (64). Interestingly, if one compares the inverted u-shaped model (see (4)) describing the effects of E/I balance on neural activity, it mirrors the classic Yerkes–Dodson law which describes an empirical relationship between arousal and behavioral performance.

In our previous studies, we reported that optogenetic inhibition of BF-PV neurons also leads to impaired 40 Hz ASSR (33) whereas phasic optogenetic stimulation can either enhance or decrease the ASSR depending on the relative time of presentation of optical and auditory stimuli (65). Taken together with our present findings, this suggests that appropriately timed synchronous activity of BF-PV neurons can enhance ASSR responses while either inappropriate inhibition or elevation of spontaneous activity of BF-PV neurons can both decrease ASSR responses. We believe this powerfully illustrates the necessity for proper E/I balance for optimal cortical processing (4 see inverted U input-output curve,5). Interestingly, prior work has shown that NMDA receptor antagonists such as ketamine and MK-801 can bidirectionally modulate ASSR (44,66), with effects critically dependent upon dosage and time post injection. Thus, the elevation of broadband gamma activity produced by our tonic BF-PV stimulation paradigm appears to better model the results observed in patients with schizophrenia, than these commonly employed pharmacological models.

To test whether impairments of task-associated gamma oscillations due to increased broadband gamma activity could also impair behavior, we additionally examined NOR task performance. Schizophrenia patients exhibit deficits in spatial working and episodic memory recognition tasks which are comparable to NOR (67,68), and this task is commonly employed as a means to develop novel treatments directed at schizophrenia-related cognitive impairment in rodent models (69). Here we observed that, despite an increase in the total number of object investigations and investigation time of both objects during familiarization, tonic BF-PV stimulation impaired not only overall NOR task performance, but also investigation induced EEG activity. The observed investigation induced activity, in the low gamma (high beta) frequency range (25–58 Hz), is consistent with increased EEG activity previously reported in mice during spatial working memory task performance (37), and has been implicated in top-down predictive coding processes (70). We observed a positive correlation between investigation induced activity and task performance, supporting the idea that impaired task-associated gamma activity is linked to impaired cognitive performance. Interestingly, we also observed a significant negative correlation between pre-investigation broadband gamma and investigation induced gamma, providing further support for the idea, described above, that increased background activity or “noise” leads to an impairment in the exploration-induced gamma response.

We have additionally observed that tonic BF-PV stimulation leads to enhanced locomotor activity, a classic schizophrenia-related behavioral phenotype in animals, similar to that observed with systemic injection of NMDA antagonists such as ketamine (71–74). Despite a weak positive correlation of this effect to broadband gamma power, this locomotor effect appears to have a different time course. Further work is needed to elucidate the mechanism underlying this effect but one possibility is that increased activity of cortical pyramidal neurons projecting to the ventral tegmental area and striatum is responsible (75). Direct projections of BF-PV neurons to motor cortex or subcortical areas involved in locomotion are another possibility (75). Interestingly, a recent study observed a similar enhancement of locomotor activity with optogenetic inhibition of GABAergic BF-somatostatin interneurons (34). Prior *in vitro* work has shown that BF-somatostatin neurons functionally inhibit BF projection neurons, including BF-PV neurons (31). Thus, inhibition of BF-somatostatin

neurons likely leads to disinhibition of BF-PV neurons, resulting in enhanced locomotor activity.

Recent findings suggest that therapeutic strategies aimed at restoration of E/I balance and associated network function may reduce symptoms in schizophrenia and improve cognitive function (4). Here, we observed that optogenetic inhibition of BF-PV neurons partially rescued the schizophrenia-like elevation in spontaneous gamma band activity elicited following acute ketamine injection. Previous work showed that direct optogenetic modulation of cortical inhibitory neuron excitability in the medial prefrontal cortex locally rescued E/I deficits (5). Our findings are consistent with that study, with the added benefit of being able to more globally modify cortical circuit activity via modulation of a small cluster of subcortical neurons. We did not observe a significant effect of optogenetic inhibition of BF-PV neurons alone on baseline levels of broadband gamma. We believe that this is largely due to the fact that background levels of broadband gamma are quite low, thus there is limited capacity to decrease this activity further. Future efforts targeting such inhibition specifically to periods with enhanced levels of broadband gamma would be of interest to resolve this issue. Alternatively, this also may be due to incomplete inhibition of BF-PV neurons using the method employed.

Several recent studies have suggested that the BF serves as a subcortical switch commanding transitions between cortical network activity associated with internally and externally focused brain states (30,34,76). Impaired suppression of default mode network (DMN) activity may represent a mechanism whereby cognitive deficits and other symptoms are induced or exacerbated in psychiatric disease (48). It has been proposed that the reciprocal relationship between DMN and task-oriented network activity is mediated via ‘net-inhibitory long-range projections’ (77,78). Informed by our prior findings (33), our present results suggest that corticopetal GABAergic BF-PV projections can robustly influence cortical gamma activity, providing a functional pathway by which BF could influence DMN activity (30). Our tonic stimulation of BF-PV neurons likely impairs the ability to functionally modulate DMN related broadband gamma activity in the cortex. This would lead to inefficiencies in the ability to actively switch between network states, required for processing task-related sensory input.

Overall, our results identify BF-PV as a critical subcortical node for regulating cortical broadband gamma activity and support the idea that enhancement in such activity leads to functional impairments in cognition and behavior. While cortical PV interneurons are well known to be impaired in schizophrenia and other neuropsychiatric disorders, little is known regarding how such disorders impact BF-PV projection neurons. These findings support future efforts to study whether there are abnormalities in BF-PV neurons in patients. Further, optogenetic inhibition of BF-PV neurons partially rescued the elevation of broadband gamma produced by subanesthetic ketamine. Thus, alteration of the activity level of BF-PV neurons may represent a novel target for therapeutic interventions to correct broadband gamma abnormalities in schizophrenia and other disorders. The paradigm presented here also provides a novel and rapidly reversible means to probe the functional consequences of altered cortical broadband gamma activity and its relationship to pathophysiology.

Supplementary Material

Refer to Web version on PubMed Central for supplementary material.

ACKNOWLEDGEMENTS:

We would like to dedicate this paper to Dr. Robert W. McCarley, who passed away on May 27th, 2017. The authors are deeply grateful for his support and his encouragement to test the ideas presented in this study which were informed by his studies of patients with schizophrenia. The work was supported by grants from VA Biomedical Laboratory and Clinical Science Research and Development Service Awards: VA CDA IK2BX002130 (JMM), IK2BX004905 (DSU), and Merit Awards I01BX004500 (JMM), I01 BX004673 (REB), I01BX001356 (REB), I01 CX001443 (KMS), I01BX002774 (RES), and NIH support from R01-MH039683 (REB), R21-NS079866 (REB), R21-NS093000 (REB), T32-MH016259 (DDA), T32-HL007901(FK&DSU) and P01-HL095491(RES). JTM received partial salary compensation and funding from Merck MISP (Merck Investigator Sponsored Programs) but has no conflict of interest with this work. JMM, JTM, DSU, KMS and REB are Research Health Scientists at VA Boston Healthcare System. The contents of this work do not represent the views of the U.S. Department of Veterans Affairs or the United States Government.

REFERENCES:

1. Rubenstein JLR, Merzenich MM. Model of autism: increased ratio of excitation/inhibition in key neural systems. Genes Brain Behav. 2003 10;2(5):255–267. [PubMed: 14606691]
2. Foss-Feig JH, Adkinson BD, Ji JL, Yang G, Srihari VH, McPartland JC, et al. Searching for Cross-Diagnostic Convergence: Neural Mechanisms Governing Excitation and Inhibition Balance in Schizophrenia and Autism Spectrum Disorders. Biol Psychiatry. 2017 5 15;81(10):848–861. [PubMed: 28434615]
3. Grossberg S The imbalanced brain: from normal behavior to schizophrenia. Biol Psychiatry. 2000 7 15;48(2):81–98. [PubMed: 10903405]
4. Krystal JH, Anticevic A, Yang GJ, Dragoi G, Driesen NR, Wang X-J, et al. Impaired tuning of neural ensembles and the pathophysiology of schizophrenia: A translational and computational neuroscience perspective. Biol Psychiatry. 2017 5 15;81(10):874–885. [PubMed: 28434616]
5. Yizhar O, Fenno LE, Prigge M, Schneider F, Davidson TJ, O'Shea DJ, et al. Neocortical excitation/inhibition balance in information processing and social dysfunction. Nature. 2011 7 27;477(7363):171–178. [PubMed: 21796121]
6. Buzsáki G, Wang X-J. Mechanisms of gamma oscillations. Annu Rev Neurosci. 2012 3 20;35:203–225. [PubMed: 22443509]
7. Gao R, Peterson EJ, Voytek B. Inferring synaptic excitation/inhibition balance from field potentials. Neuroimage. 2017 7 1;158:70–78. [PubMed: 28676297]
8. Llinás RR, Ribary U, Jeanmonod D, Kronberg E, Mitra PP. Thalamocortical dysrhythmia: A neurological and neuropsychiatric syndrome characterized by magnetoencephalography. Proc Natl Acad Sci USA. 1999 12 21;96(26):15222–15227. [PubMed: 10611366]
9. Grent-'t-Jong T, Gross J, Goense J, Wibral M, Gajwani R, Gumley AI, et al. Resting-state gamma-band power alterations in schizophrenia reveal E/I-balance abnormalities across illness-stages. Elife. 2018 9 27;7.
10. Baradits M, Kakuszi B, Bálint S, Fullajtár M, Mód L, Bitter I, et al. Alterations in resting-state gamma activity in patients with schizophrenia: a high-density EEG study. Eur Arch Psychiatry Clin Neurosci. 2019 6;269(4):429–437. [PubMed: 29569047]
11. Hirano Y, Oribe N, Kanba S, Onitsuka T, Nestor PG, Spencer KM. Spontaneous gamma activity in schizophrenia. JAMA Psychiatry. 2015 8;72(8):813–821. [PubMed: 25587799]
12. Spencer KM. Baseline gamma power during auditory steady-state stimulation in schizophrenia. Front Hum Neurosci. 2011;5:190. [PubMed: 22319485]
13. Pinault D N-methyl d-aspartate receptor antagonists ketamine and MK-801 induce wake-related aberrant gamma oscillations in the rat neocortex. Biol Psychiatry. 2008 4 15;63(8):730–735. [PubMed: 18022604]

14. McNally JM, McCarley RW, McKenna JT, Yanagawa Y, Brown RE. Complex receptor mediation of acute ketamine application on in vitro gamma oscillations in mouse prefrontal cortex: modeling gamma band oscillation abnormalities in schizophrenia. Neuroscience. 2011 12 29;199:51–63. [PubMed: 22027237]
15. Kocsis B Differential role of NR2A and NR2B subunits in N-methyl-D-aspartate receptor antagonist-induced aberrant cortical gamma oscillations. Biol Psychiatry. 2012 6 1;71(11):987–995. [PubMed: 22055014]
16. Rivolta D, Heidegger T, Scheller B, Sauer A, Schaum M, Birkner K, et al. Ketamine Dysregulates the Amplitude and Connectivity of High-Frequency Oscillations in Cortical-Subcortical Networks in Humans: Evidence From Resting-State Magnetoencephalography-Recordings. Schizophr Bull. 2015 9;41(5):1105–1114. [PubMed: 25987642]
17. Muthukumaraswamy SD, Shaw AD, Jackson LE, Hall J, Moran R, Saxena N. Evidence that Subanesthetic Doses of Ketamine Cause Sustained Disruptions of NMDA and AMPA-Mediated Frontoparietal Connectivity in Humans. J Neurosci. 2015 8 19;35(33):11694–11706. [PubMed: 26290246]
18. Grent-'t-Jong T, Rivolta D, Gross J, Gajwani R, Lawrie SM, Schwannauer M, et al. Acute ketamine dysregulates task-related gamma-band oscillations in thalamo-cortical circuits in schizophrenia. Brain. 2018 8 1;141(8):2511–2526. [PubMed: 30020423]
19. Homayoun H, Moghaddam B. Orbitofrontal cortex neurons as a common target for classic and glutamatergic antipsychotic drugs. Proc Natl Acad Sci USA. 2008 11 18;105(46):18041–18046. [PubMed: 19004793]
20. Grunze HC, Rainnie DG, Hasselmo ME, Barkai E, Hearn EF, McCarley RW, et al. NMDA-dependent modulation of CA1 local circuit inhibition. J Neurosci. 1996 3 15;16(6):2034–2043. [PubMed: 8604048]
21. Gandal MJ, Anderson RL, Billingslea EN, Carlson GC, Roberts TPL, Siegel SJ. Mice with reduced NMDA receptor expression: more consistent with autism than schizophrenia? Genes Brain Behav. 2012 8;11(6):740–750. [PubMed: 22726567]
22. White RS, Siegel SJ. Cellular and circuit models of increased resting-state network gamma activity in schizophrenia. Neuroscience. 2016 5 3;321:66–76. [PubMed: 26577758]
23. Carlén M, Meletis K, Siegle JH, Cardin JA, Futai K, Vierling-Claassen D, et al. A critical role for NMDA receptors in parvalbumin interneurons for gamma rhythm induction and behavior. Mol Psychiatry. 2012 5;17(5):537–548. [PubMed: 21468034]
24. Cape EG, Jones BE. Differential modulation of high-frequency gamma-electroencephalogram activity and sleep-wake state by noradrenaline and serotonin microinjections into the region of cholinergic basalis neurons. J Neurosci. 1998 4 1;18(7):2653–2666. [PubMed: 9502823]
25. Cape EG, Jones BE. Effects of glutamate agonist versus procaine microinjections into the basal forebrain cholinergic cell area upon gamma and theta EEG activity and sleep-wake state. Eur J Neurosci. 2000 6;12(6):2166–2184. [PubMed: 10886356]
26. Buzsaki G, Bickford RG, Ponomareff G, Thal LJ, Mandel R, Gage FH. Nucleus basalis and thalamic control of neocortical activity in the freely moving rat. J Neurosci. 1988 11;8(11):4007–4026. [PubMed: 3183710]
27. Kaur S, Junek A, Black MA, Semba K. Effects of ibotenate and 192IgG-saporin lesions of the nucleus basalis magnocellularis/substantia innominata on spontaneous sleep and wake states and on recovery sleep after sleep deprivation in rats. J Neurosci. 2008 1 9;28(2):491–504. [PubMed: 18184792]
28. Fuller PM, Sherman D, Pedersen NP, Saper CB, Lu J. Reassessment of the structural basis of the ascending arousal system. J Comp Neurol. 2011 4 1;519(5):933–956. [PubMed: 21280045]
29. Nair J, Klaassen A-L, Poirot J, Vyssotski A, Rasch B, Rainer G. Gamma band directional interactions between basal forebrain and visual cortex during wake and sleep states. J Physiol Paris. 2016 11 29;110(1–2):19–28. [PubMed: 27913167]
30. Nair J, Klaassen A-L, Arato J, Vyssotski AL, Harvey M, Rainer G. Basal forebrain contributes to default mode network regulation. Proc Natl Acad Sci USA. 2018 2 6;115(6):1352–1357. [PubMed: 29363595]

31. Xu M, Chung S, Zhang S, Zhong P, Ma C, Chang W-C, et al. Basal forebrain circuit for sleep-wake control. Nat Neurosci. 2015 11;18(11):1641–1647. [PubMed: 26457552]
32. Anaclet C, Pedersen NP, Ferrari LL, Venner A, Bass CE, Arrigoni E, et al. Basal forebrain control of wakefulness and cortical rhythms. Nat Commun. 2015 11 3;6:8744. [PubMed: 26524973]
33. Kim T, Thankachan S, McKenna JT, McNally JM, Yang C, Choi JH, et al. Cortically projecting basal forebrain parvalbumin neurons regulate cortical gamma band oscillations. Proc Natl Acad Sci USA. 2015 3 17;112(11):3535–3540. [PubMed: 25733878]
34. Espinosa N, Alonso A, Morales C, Espinosa P, Chávez AE, Fuentealba P. Basal forebrain gating by somatostatin neurons drives prefrontal cortical activity. Cereb Cortex. 2019 1 1;29(1):42–53. [PubMed: 29161383]
35. McKenna JT, Yang C, Franciosi S, Winston S, Abarr KK, Rigby MS, et al. Distribution and intrinsic membrane properties of basal forebrain GABAergic and parvalbumin neurons in the mouse. J Comp Neurol. 2013 4 15;521(6):1225–1250. [PubMed: 23254904]
36. Prerau MJ, Brown RE, Bianchi MT, Ellenbogen JM, Purdon PL. Sleep neurophysiological dynamics through the lens of multitaper spectral analysis. Physiology (Bethesda). 2017;32(1):60–92. [PubMed: 27927806]
37. Zhang RV, Featherstone RE, Melynchenko O, Gifford R, Weger R, Liang Y, et al. High-beta/low-gamma frequency activity reflects top-down predictive coding during a spatial working memory test. Exp Brain Res. 2019 5 15;1–8.
38. Bakdash JZ, Marusich LR. Repeated Measures Correlation. Front Psychol. 2017 4 7;8:456. [PubMed: 28439244]
39. Kwon JS, O'Donnell BF, Wallenstein GV, Greene RW, Hirayasu Y, Nestor PG, et al. Gamma frequency-range abnormalities to auditory stimulation in schizophrenia. Arch Gen Psychiatry. 1999 11;56(11):1001–1005. [PubMed: 10565499]
40. Thuné H, Recasens M, Uhlhaas PJ. The 40-Hz Auditory Steady-State Response in Patients With Schizophrenia: A Meta-analysis. JAMA Psychiatry. 2016 11 1;73(11):1145–1153. [PubMed: 27732692]
41. Brenner CA, Krishnan GP, Vohs JL, Ahn W-Y, Hetrick WP, Morzorati SL, et al. Steady state responses: electrophysiological assessment of sensory function in schizophrenia. Schizophr Bull. 2009 11;35(6):1065–1077. [PubMed: 19726534]
42. Light GA, Hsu JL, Hsieh MH, Meyer-Gomes K, Sprock J, Swerdlow NR, et al. Gamma band oscillations reveal neural network cortical coherence dysfunction in schizophrenia patients. Biol Psychiatry. 2006 12 1;60(11):1231–1240. [PubMed: 16893524]
43. Nakao K, Nakazawa K. Brain state-dependent abnormal LFP activity in the auditory cortex of a schizophrenia mouse model. Front Neurosci. 2014 7 1;8:168. [PubMed: 25018691]
44. Sivarao DV. The 40-Hz auditory steady-state response: a selective biomarker for cortical NMDA function. Ann N Y Acad Sci. 2015 5;1344:27–36. [PubMed: 25809615]
45. Curic S, Leicht G, Thiebes S, Andreou C, Polomac N, Eichler I-C, et al. Reduced auditory evoked gamma-band response and schizophrenia-like clinical symptoms under subanesthetic ketamine. Neuropsychopharmacology. 2019 2 6;44(7):1239–1246. [PubMed: 30758327]
46. Leger M, Quiedeville A, Bouet V, Haelewyn B, Boulouard M, Schumann-Bard P, et al. Object recognition test in mice. Nat Protoc. 2013 12;8(12):2531–2537. [PubMed: 24263092]
47. Hakami T, Jones NC, Tolmacheva EA, Gaudias J, Chaumont J, Salzberg M, et al. NMDA receptor hypofunction leads to generalized and persistent aberrant gamma oscillations independent of hyperlocomotion and the state of consciousness. PLoS One. 2009 8 25;4(8):e6755. [PubMed: 19707548]
48. Anticevic A, Cole MW, Murray JD, Corlett PR, Wang X-J, Krystal JH. The role of default network deactivation in cognition and disease. Trends Cogn Sci (Regul Ed). 2012 12;16(12):584–592.
49. Allen P, Sommer IE, Jardri R, Eysenck MW, Hugdahl K. Extrinsic and default mode networks in psychiatric conditions: Relationship to excitatory-inhibitory transmitter balance and early trauma. Neurosci Biobehav Rev. 2019 2 12;99:90–100. [PubMed: 30769024]
50. Détári L, Rasmusson DD, Semba K. The role of basal forebrain neurons in tonic and phasic activation of the cerebral cortex. Prog Neurobiol. 1999 6;58(3):249–277. [PubMed: 10341363]

51. Zaborszky L, Duque A. Sleep-wake mechanisms and basal forebrain circuitry. Front Biosci. 2003 9 1;8:d1146–69. [PubMed: 12957822]
52. Lin S-C, Brown RE, Hussain Shuler MG, Petersen CCH, Kepecs A. Optogenetic dissection of the basal forebrain neuromodulatory control of cortical activation, plasticity, and cognition. J Neurosci. 2015 10 14;35(41):13896–13903. [PubMed: 26468190]
53. Yang C, Thankachan S, McCarley RW, Brown RE. The menagerie of the basal forebrain: how many (neural) species are there, what do they look like, how do they behave and who talks to whom? Curr Opin Neurobiol. 2017 5 21;44:159–166. [PubMed: 28538168]
54. Berridge CW, Foote SL. Enhancement of behavioral and electroencephalographic indices of waking following stimulation of noradrenergic beta-receptors within the medial septal region of the basal forebrain. J Neurosci. 1996 11 1;16(21):6999–7009. [PubMed: 8824336]
55. Goard M, Dan Y. Basal forebrain activation enhances cortical coding of natural scenes. Nat Neurosci. 2009 11;12(11):1444–1449. [PubMed: 19801988]
56. Thankachan S, Katsuki F, McKenna JT, Yang C, Shukla C, Deisseroth K, et al. Thalamic reticular nucleus parvalbumin neurons regulate sleep spindles and electrophysiological aspects of schizophrenia in mice. Sci Rep. 2019 3 5;9(1):3607. [PubMed: 30837664]
57. Orekhova EV, Stroganova TA, Nygren G, Tsetlin MM, Posikera IN, Gillberg C, et al. Excess of high frequency electroencephalogram oscillations in boys with autism. Biol Psychiatry. 2007 11 1;62(9):1022–1029. [PubMed: 17543897]
58. Rojas DC, Maharajh K, Teale P, et al. Reduced neural synchronization of gamma-band MEG oscillations in first-degree relatives of children with autism. BMC …. 2008;
59. Winterer G, Coppola R, Goldberg TE, Egan MF, Jones DW, Sanchez CE, et al. Prefrontal broadband noise, working memory, and genetic risk for schizophrenia. Am J Psychiatry. 2004 3;161(3):490–500. [PubMed: 14992975]
60. Parker DA, Hamm JP, McDowell JE, Keedy SK, Gershon ES, Ivleva EI, et al. Auditory steady-state EEG response across the schizo-bipolar spectrum. Schizophr Res. 2019 7;209:218–226. [PubMed: 31080153]
61. Rosburg T, Boutros NN, Ford JM. Reduced auditory evoked potential component N100 in schizophrenia--a critical review. Psychiatry Res. 2008 12 15;161(3):259–274. [PubMed: 18926573]
62. Salisbury DF, Collins KC, McCarley RW. Reductions in the N1 and P2 auditory event-related potentials in first-hospitalized and chronic schizophrenia. Schizophr Bull. 2010 9;36(5):991–1000. [PubMed: 19282472]
63. Ahveninen J, Jääskeläinen IP, Osipova D, Huttunen MO, Ilmoniemi RJ, Kaprio J, et al. Inherited auditory-cortical dysfunction in twin pairs discordant for schizophrenia. Biol Psychiatry. 2006 9 15;60(6):612–620. [PubMed: 16876141]
64. McKenna JT, Thankachan S, Uygun DS, Shukla C, McNally JM, Schiffino FL, et al. Basal Forebrain Parvalbumin Neurons Mediate Arousals from Sleep Induced by Hypercarbia or Auditory Stimuli. Curr Biol. 2020 4 30;
65. Hwang E, Brown RE, Kocsis B, Kim T, McKenna JT, McNally JM, et al. Optogenetic stimulation of basal forebrain parvalbumin neurons modulates the cortical topography of auditory steady-state responses. Brain Struct Funct. 2019 5;224(4):1505–1518. [PubMed: 30826928]
66. Sullivan EM, Timi P, Hong LE, O'Donnell P. Effects of NMDA and GABA-A Receptor Antagonism on Auditory Steady-State Synchronization in Awake Behaving Rats. Int J Neuropsychopharmacol. 2015 1 2;18(7):pyu118. [PubMed: 25556198]
67. Tek C, Gold J, Blaxton T, Wilk C, McMahon RP, Buchanan RW. Visual perceptual and working memory impairments in schizophrenia. Arch Gen Psychiatry. 2002 2;59(2):146–153. [PubMed: 11825136]
68. Heckers S, Curran T, Goff D, Rauch SL, Fischman AJ, Alpert NM, et al. Abnormalities in the thalamus and prefrontal cortex during episodic object recognition in schizophrenia. Biol Psychiatry. 2000 10 1;48(7):651–657. [PubMed: 11032976]
69. Rajagopal L, Massey BW, Huang M, Oyamada Y, Meltzer HY. The novel object recognition test in rodents in relation to cognitive impairment in schizophrenia. Curr Pharm Des. 2014;20(31):5104–5114. [PubMed: 24345269]

70. Bastos AM, Usrey WM, Adams RA, Mangun GR, Fries P, Friston KJ. Canonical microcircuits for predictive coding. Neuron. 2012 11 21;76(4):695–711. [PubMed: 23177956]

71. Dugladze T, Lepsveridze E, Breustedt J, Kehrer C, Heinemann U, Gloveli T. Effects of phencyclidines on signal transfer from the entorhinal cortex to the hippocampus in rats. Neurosci Lett. 2004 1 16;354(3):185–188. [PubMed: 14700727]

72. Gloveli T, Iserhot C, Schmitz D, Castrén E, Behr J, Heinemann U. Systemic administration of the phencyclidine compound MK-801 affects stimulus-induced field potentials selectively in layer III of rat medial entorhinal cortex. Neurosci Lett. 1997 1 17;221(2–3):93–96. [PubMed: 9121708]

73. Kehrer C, Dugladze T, Maziashvili N, Wójtowicz A, Schmitz D, Heinemann U, et al. Increased inhibitory input to CA1 pyramidal cells alters hippocampal gamma frequency oscillations in the MK-801 model of acute psychosis. Neurobiol Dis. 2007 3;25(3):545–552. [PubMed: 17169567]

74. Väisänen J, Lindén AM, Lakso M, Wong G, Heinemann U, Castrén E. Excitatory actions of NMDA receptor antagonists in rat entorhinal cortex and cultured entorhinal cortical neurons. Neuropsychopharmacology. 1999 7;21(1):137–146. [PubMed: 10379528]

75. Do JP, Xu M, Lee S-H, Chang W-C, Zhang S, Chung S, et al. Cell type-specific long-range connections of basal forebrain circuit. Elife. 2016 9 19;5.

76. Espinosa N, Alonso A, Lara-Vasquez A, Fuentealba P. Basal forebrain somatostatin cells differentially regulate local gamma oscillations and functionally segregate motor and cognitive circuits. Sci Rep. 2019 2 22;9(1):2570. [PubMed: 30796293]

77. Hayden BY, Smith DV, Platt ML. Electrophysiological correlates of default-mode processing in macaque posterior cingulate cortex. Proc Natl Acad Sci USA. 2009 4 7;106(14):5948–5953. [PubMed: 19293382]

78. Anticevic A, Gancsos M, Murray JD, Repovs G, Driesen NR, Ennis DJ, et al. NMDA receptor function in large-scale anticorrelated neural systems with implications for cognition and schizophrenia. Proc Natl Acad Sci USA. 2012 10 9;109(41):16720–16725. [PubMed: 23012427]

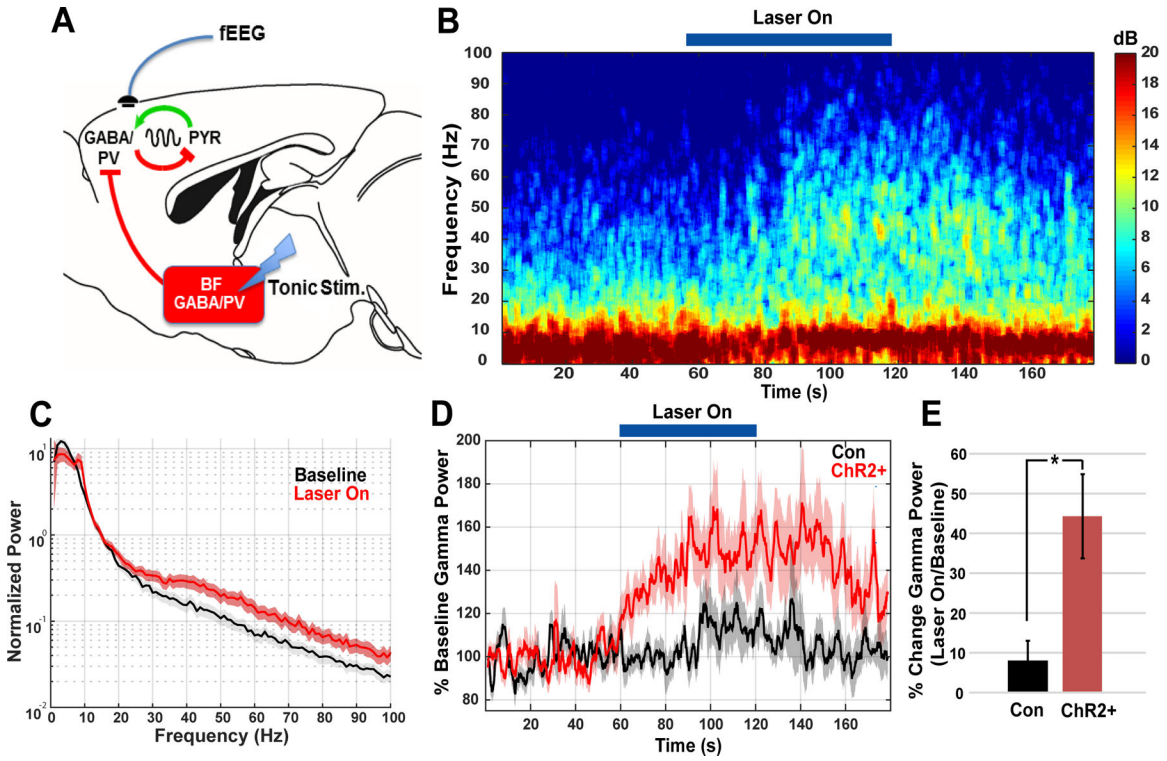

Figure 1: Tonic optical stimulation of basal forebrain (BF) parvalbumin (PV) neurons increases broadband cortical gamma band (30–80 Hz) activity, a measure of cortical excitatory-inhibitory (E/I) balance.

(A) Schematic of the experiment. The sagittal brain section shows the location of the BF-PV neurons transduced with channelrhodopsin 2 (ChR2), allowing optical stimulation using blue light and the frontal electroencephalographic (EEG) recording site. BF-PV neurons project to cortical GABAergic interneurons, including those which contain PV, allowing BF-PV neurons to influence cortical activity via reciprocal circuit interactions with cortical pyramidal neurons (PYR). BF-PV projections to the thalamic reticular nucleus ((56), not shown) are another potential route by which BF-PV neurons may modulate cortical activity; **(B)** Representative averaged time frequency spectrogram of cortical EEG activity shows the effect of tonic, low wattage bilateral optogenetic stimulation of BF-PV neurons (60 s of constant 5 mW laser light). This stimulus elicited a robust and progressive elevation of broadband power across the gamma frequency range, which was maintained beyond cessation of stimulation. **(C)** For mice expressing ChR2, a comparison of the overall power spectral density for the 60 s period prior to stimulation (baseline) to that observed during stimulation (Laser On) showed an elevation in power across the gamma frequency range (30–100Hz), as well as a moderate enhancement in theta (6–10 Hz). **(D&E)** Across all experimental animals, tonic stimulation (60–120 s) significantly elevated EEG power in the gamma band (30–80 Hz), when compared to background (0–60 s). This effect was specific for mice expressing ChR2 in BF-PV neurons (ChR2+, (N=12), and was not observed in controls which received laser stimulation alone (Con, N=8). (*p<0.05; paired t-test).

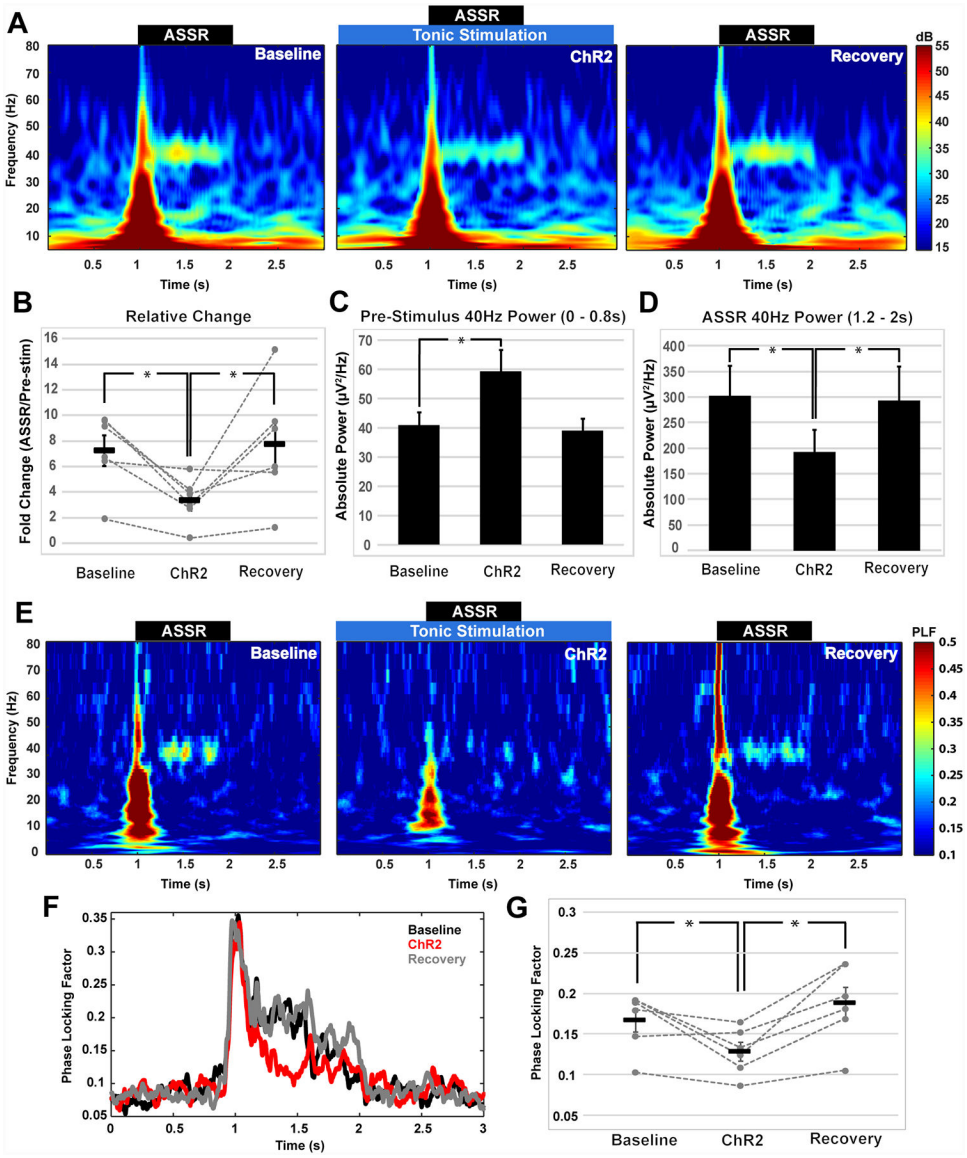

Figure 2: Elevation of broadband gamma activity by tonic optical stimulation of BF-PV neurons impairs the 40 Hz auditory steady-state response (ASSR).

ASSR is a measure of the ability of the cortex to generate evoked narrowband cortical gamma oscillations which is impaired in schizophrenia. Mice received three consecutive blocks of 40 Hz trains of auditory stimulation. The first ASSR block provided a baseline measure of the cortical response to auditory stimuli and consisted of 100 repetitions of a 1 s train of clicks delivered at 90 dB. For the second ASSR block, auditory stimulation was combined with constant low wattage (5 mW) optogenetic stimulation of BF-PV neurons. Finally, mice received a third ASSR block of auditory stimulation alone, to assess recovery from optogenetic stimulation. **(A)** Grand average time frequency spectrograms show the EEG response to 40 Hz auditory stimulation in frontal cortex, under each condition. **(B)** Comparison of the relative change at 40 Hz (±5Hz) power shows a significant impairment when auditory stimulation was coupled with tonic BF-PV stimulation, which recovers to baseline levels following cessation of optogenetic stimuli (N=6). Results from individual

mice are plotted with dashed lines, with the mean represented by black bars with SEM. **(C & D)** This impairment results from both an elevation in the absolute power of background 40 Hz activity, calculated from the period preceding the auditory stimuli (0 – 0.8s, panel C), as well as a significant decrease in the absolute value of evoked 40 Hz power (1.2 – 2s, panel D). (*p<0.05; RMANOVA with Tukey's HSD post hoc). Phase locking factor (PLF) was additionally assessed from ASSR data. **(E)** Grand average spectrograms show phase locking factor response to 40 Hz auditory stimulation in frontal cortex under baseline, tonic stimulation, and recovery conditions. **(F)** Comparison of PLF at 40 Hz (±2Hz) under each condition, shows that when auditory stimuli were coupled with tonic BF-PV stimulation, PLF was reduced, and recovered to baseline levels following cessation of optogenetic stimuli (N=6). **(G)** The mean PLF during auditory stimuli (1–2s) calculated for individual mice are plotted with dashed lines, which shows a significant reduction in 40Hz PLF during the tonic BF-PV stimulation block, compared to baseline and recovery. The mean across all animals tested represented by black bars with SEM. (*p<0.05; RMANOVA with Tukey's HSD post hoc).

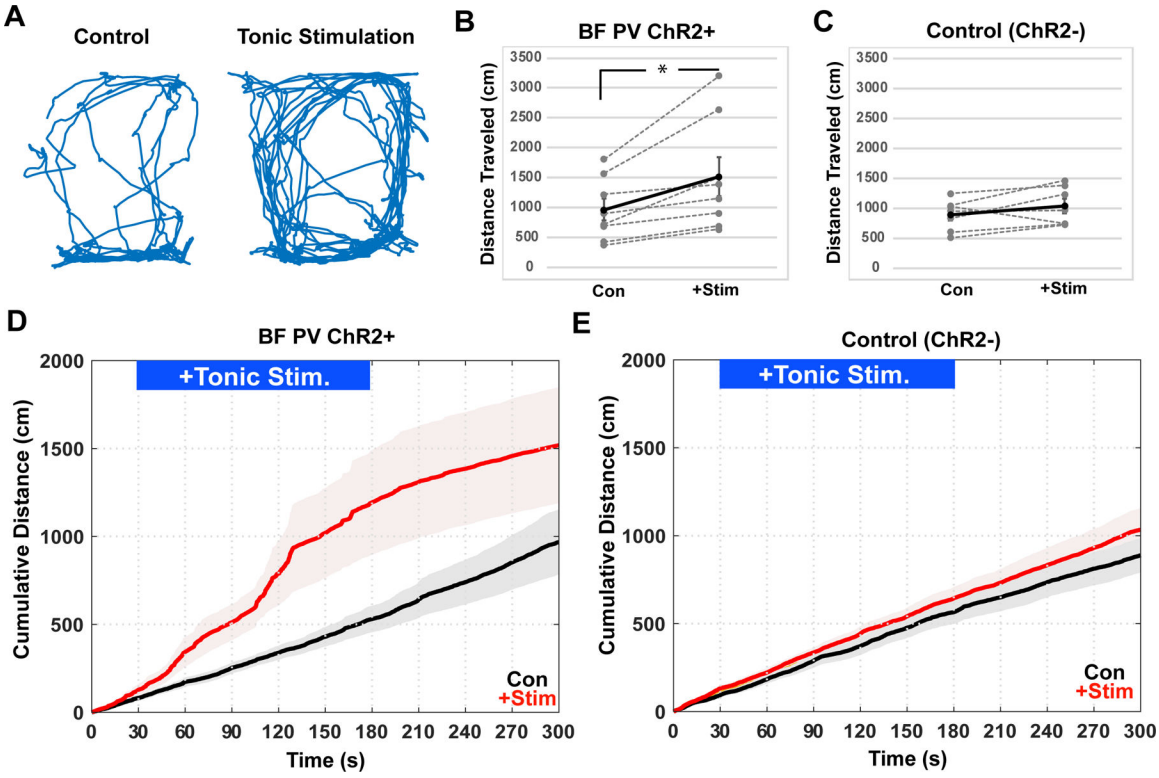

Figure 3: Tonic optical stimulation of BF-PV neurons increases open field locomotor activity.

Locomotor activity in an open field environment was tracked across a 5-minute period in mice expressing channelrhodopsin2 (ChR2) in BF-PV neurons (BF-PV ChR2+) and control animals (ChR2-), both with and without tonic optogenetic stimulation (2.5 min tonic stimulation at 5 mW; blue bar). **(A)** Representative example demonstrating the effect of tonic optogenetic stimulation on locomotor activity in a mouse expressing ChR2. **(B&C)** Mice expressing ChR2 (ChR2+, N=8) showed a significant increase in total distance traveled across the 5 minutes of the experiment. This was not observed in animals which did not express ChR2 (ChR2-, N=6). **(D & E)** Cumulative distance traveled plots for ChR2+ and ChR2- mice show that increased locomotor activity corresponded with expression of ChR2 in BF-PV neurons. Thus, this effect was not due to non-specific effects of the blue light delivered to the BF. (*p<0.05; paired t test).

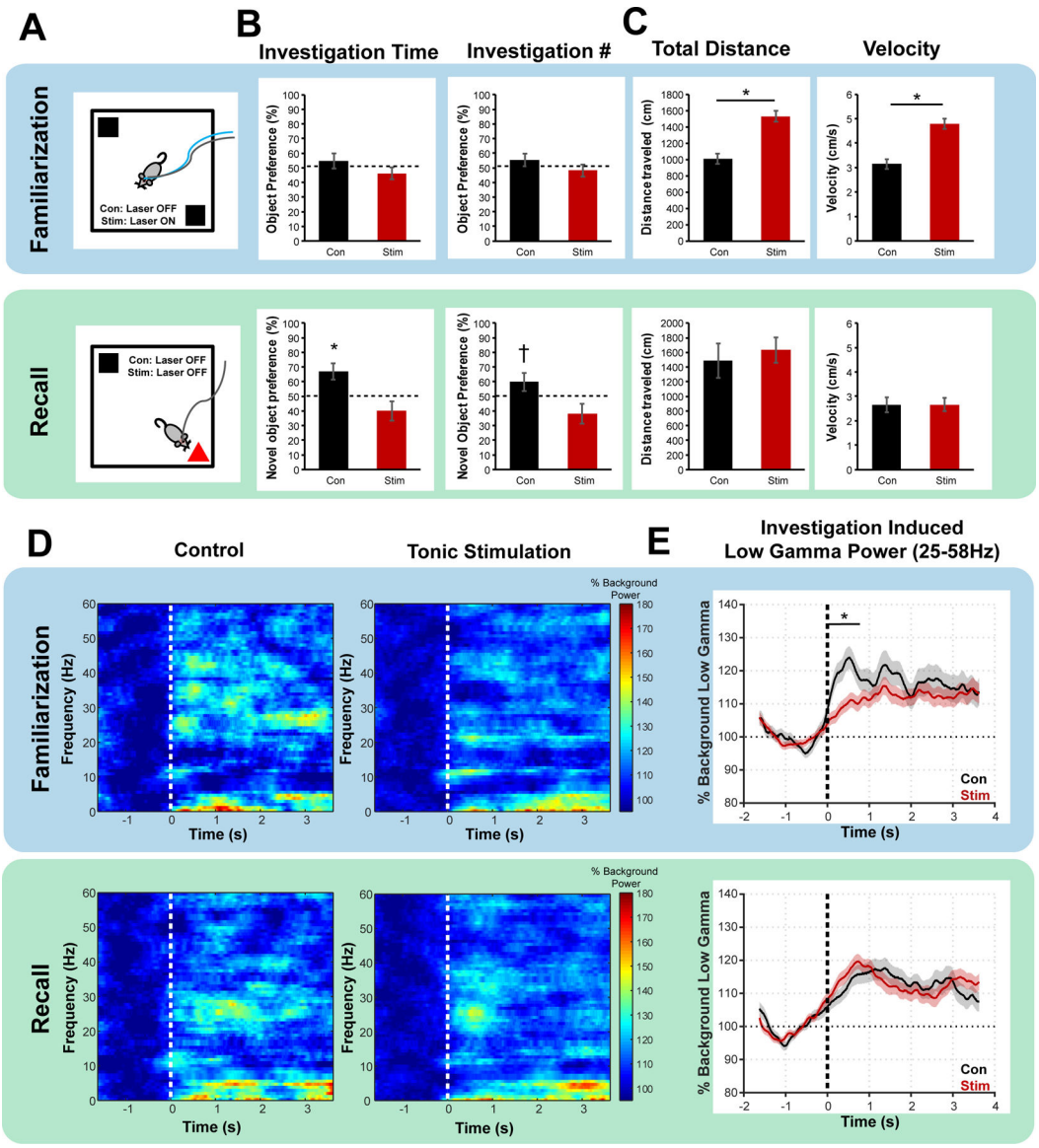

Figure 4: Elevation of broadband gamma activity by tonic optical stimulation of BF-PV neurons impairs working memory in the NOR task and object investigation induced gamma band activity.

(A) NOR task performance was assessed in mice expressing channelrhodopsin2 (ChR2) in BF-PV neurons, with and without bilateral tonic low wattage (5 mW) optogenetic stimulation given during the familiarization phase of the task. **(B)** No difference was observed between these groups in object preference during the familiarization phase of the task in terms of the % of the overall number of investigations, and % of total investigation time. During the recall phase, novel object preference was observed only in controls, and not in mice which had received BF-PV stimulation during the familiarization period (Univariate t-test: * denotes $p<0.05$, and † denotes $p<0.10$). **(C)** BF-PV stimulation significantly increased locomotor activity during the familiarization phase of the task, which returned to control levels during the recall phase (*$p<0.05$; paired t test). **(D)** Time frequency plots show the grand average of investigation induced frontal EEG activity for both control and BF-PV

tonic stimulation groups for both familiarization and recall phases of the task. Spectral analysis of EEG activity related to object investigation (dashed line) was performed, with results normalized and pooled across all experimental animals (n = 10) for each phase of the task and treatment group (Control Familiarization: n = 80; Stim Familiarization: n = 163; Control Recall: n = 107; Recall following Stim: n = 174). Investigation induced activity was observed in the lower gamma band range (~25–58Hz). **(E)** Analysis of activity at this range across all groups and task phases shows a robust investigation induced gamma response in control mice during the familiarization phase of the task which is significantly impaired with concurrent BF-PV stimulation. Investigation induced gamma was restored to control levels during the recall phase, in the absence of BF PV stimulation. (*$p<0.05$; RMANOVA with Tukey's HSD post hoc)

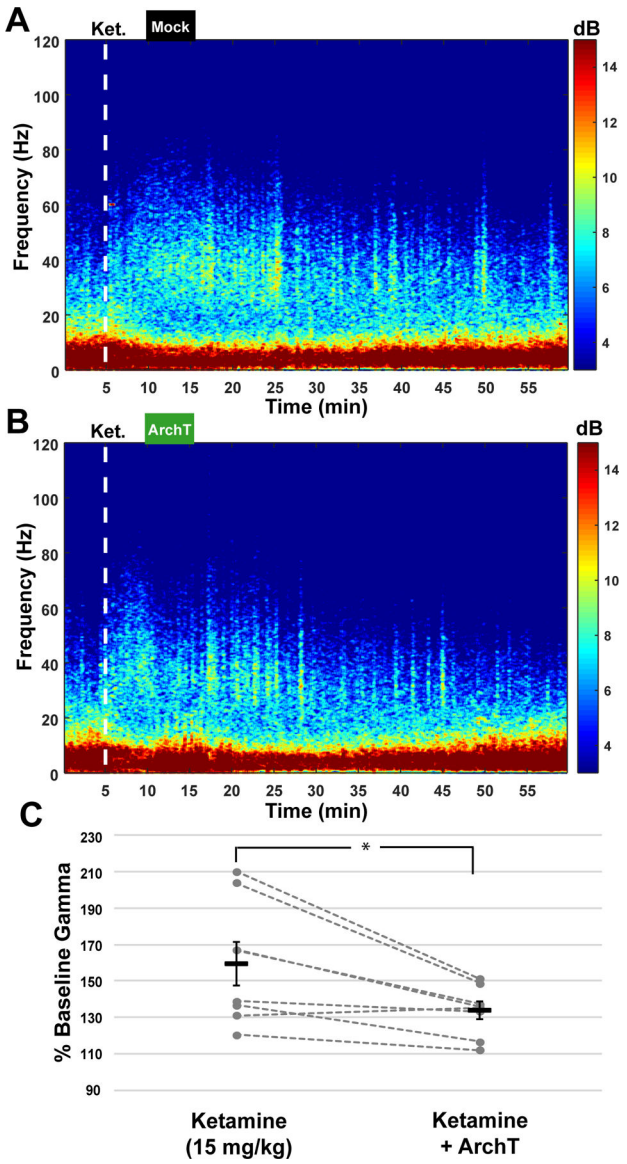

Figure 5: Optogenetic inhibition of BF-PV neurons partially rescues the elevation in broadband gamma activity caused by the psychotomimetic drug, ketamine.

Mice expressing the inhibitory proton pump, Archaerhodopsin TP003 (ArchT), in BF-PV neurons were given an acute injection of ketamine (15 mg/kg i.p.) to elicit an increase in spontaneous gamma activity. Five minutes following this injection, mice received 5 minutes of mock BF-PV stimulation (Laser Off), or bilateral tonic optogenetic inhibition (20 mW). **(A & B)** Representative time frequency spectrograms show the broadband elevation in gamma band activity following ketamine injection (dotted white line). This elevation in spontaneous gamma was reversibly diminished with optogenetic inhibition of BF-PV neurons (green bar). This was not observed with mock stimulation (ketamine alone) in the same mice. **(C)** For each mouse tested (N=7), the percent increase in gamma band power (30–80 Hz) elicited by ketamine was calculated across a 5-minute period (600–900s) during ArchT or mock inhibition. Mice showed a significant decrease in the ketamine-elicited

increase in spontaneous gamma with ArchT inhibition compared to mock stimulation. (*$p<0.05$; paired t test).